

THE SUZAKU VIEW OF THE DISK-JET CONNECTION IN THE LOW EXCITATION RADIO GALAXY NGC 6251

D. A. EVANS^{1,2}, A. C. SUMMERS², M. J. HARDCASTLE³, R. P. KRAFT¹, P. GANDHI⁴, J. H. CROSTON⁵, J. C. LEE¹

Draft version September 30, 2011

ABSTRACT

We present results from an 87-ks *Suzaku* observation of the canonical low-excitation radio galaxy (LERG) NGC 6251. We have previously suggested that LERGs violate conventional AGN unification schemes: they may lack an obscuring torus and are likely to accrete in a radiatively inefficient manner, with almost all of the energy released by the accretion process being channeled into powerful jets. We model the 0.5–20 keV *Suzaku* spectrum with a single power law of photon index $\Gamma = 1.82^{+0.04}_{-0.05}$, together with two collisionally ionized plasma models whose parameters are consistent with the known galaxy- and group-scale thermal emission. Our observations confirm that there are no signatures of obscured, accretion-related X-ray emission in NGC 6251, and we show that the luminosity of any such component must be substantially sub-Eddington in nature.

Subject headings: galaxies: active – galaxies: jets – galaxies: individual (NGC 6251) – X-rays: galaxies

1. INTRODUCTION

The origin of relativistic jets in active galactic nuclei (AGN) is a key unsolved problem in extragalactic astrophysics. While 90% of all AGN (Seyfert galaxies and radio-quiet quasars) show little or no jet emission, the remaining 10% (the radio-loud AGN and radio-loud quasars) launch powerful twin jets of particles from their cores. Since jets transport a significant fraction of the energy liberated during the accretion process, sometimes out to \sim Mpc distances, understanding how they are produced is critical to a complete picture of accretion and feedback in AGN.

X-ray observations of the nuclei of radio-loud AGN are particularly useful for establishing the connection between the accretion flow, black hole, and jet. Since the launch of *Chandra* and *XMM-Newton*, several groups have performed spectroscopic studies of the nuclei of 3CRR radio galaxies (e.g., Evans et al. 2006; Balmaverde et al. 2006; Hardcastle et al. 2007, 2009). These efforts have found a dichotomy in the nuclear X-ray spectra of radio-loud AGN, related to the optical emission line classifications, which may be related to their differing roles of hot and cold gas accretion (Hardcastle et al. 2007), or possibly the spin configuration of the black hole itself (Garofalo et al. 2010).

High-excitation radio galaxies (HERGs), those with prominent emission lines in their optical spectra, have X-ray spectra that are consistent with unification models. HERGs have standard, cool luminous accretion disks and strong (yet typically unbroadened) Fe K α lines. The nuclear continuum is heavily obscured in the X-ray by cold gas with columns of $\sim 10^{23}$ cm⁻² (Evans et al. 2006) when the source AGN is viewed close to edge-on with respect to the observer, and are largely unobscured when oriented closer to the line of sight. These sources also have an additional component of unabsorbed

emission that is associated with the pc-scale jet. HERGs tend to occupy gas-poor environments (e.g., Kraft et al. 2007) and their host galaxies lie in the ‘green valley’ of the galaxy color-mass diagram (Smolčić 2009).

Low-excitation radio galaxies (LERGs), on the other hand, the population of radio-loud AGN with little or no nuclear optical line emission, *seem to lack any of the features required by standard AGN unification models*. We have previously argued that their X-ray emission is dominated by radiation from a parsec-scale jet, that they have no signatures of standard, cold accretion disks, and that they may show no evidence at all for an obscuring torus (Ogle et al. 2006; Hardcastle et al. 2009). We have suggested that accretion in LERGs takes place in a radiatively inefficient manner, with almost all the available energy from accretion being channeled into jets. LERG host galaxies lie in the red sequence on the color-mass diagram (Smolčić 2009) and are often associated with group- or cluster-scale hot-gas environments (e.g., Tasse et al. 2008).

Constraining the properties of the accretion flow in LERGs with deep X-ray observations would provide a strong test of our hypothesis that the X-ray emission is dominated by a jet with no signatures of cold-gas accretion. However, existing observations of LERGs have been restricted to relatively poor signal-to-noise *Chandra* and *XMM-Newton* data, while the >10 keV band where the Compton reflection hump could lie is completely inaccessible to those observatories. In order to address these issues, we obtained an 87-ks *Suzaku* observation of NGC 6251 ($z=0.0247$), the X-ray brightest low-excitation radio galaxy in the 3CRR catalog. We use the XIS and HXD to search for signatures that are related to a standard, cool accretion disk that is surrounded by a torus: (1) a ~ 6.4 keV Fe K α line, (2) heavily absorbed continuum emission, and (3) the >10 keV Compton reflection hump (George & Fabian 1991). Detection of any of these features would immediately invalidate our model.

Previous attempts to understand the origin of X-ray emission in NGC 6251 have yielded conflicting results, making our *Suzaku* observation particularly useful. For example, Turner et al. (1997) (based on ASCA data) and Gliozzi et al. (2004) (based on *XMM-Newton* data) claimed a detection of a high-equivalent width Fe K α line, suggestive of a dominant contribution from a luminous accretion disk. However, reanalysis of the *XMM-Newton* spectra by Evans et al.

¹ Harvard-Smithsonian Center for Astrophysics, 60 Garden Street, Cambridge, MA 02138

² Elon University, 100 Campus Drive, Elon, NC 27244

³ School of Physics, Astronomy & Mathematics, University of Hertfordshire, College Lane, Hatfield AL10 9AB, UK

⁴ Institute of Space and Astronautical Science (ISAS), Japan Aerospace Exploration Agency, 3-1-1 Yoshinodai, Chuo-ku, Sagami-hara 252-5210, Japan

⁵ School of Physics and Astronomy, University of Southampton, Southampton, SO17 1BJ, UK

(2005) instead showed no evidence of an Fe $K\alpha$ line, which favors a jet-dominated scenario. Furthermore, the double-peaked SED of NGC 6251 measured by, e.g., Ho (1999), Guainazzi et al. (2003), Chiaberge et al. (2003), Evans et al. (2005), and Migliori et al. (2011) led those authors to conclude that the high-energy emission is synchrotron self-Compton (SSC) emission from a jet. Finally, analysis of the spectral variability from a long-term monitoring campaign with *RXTE* (Gliozzi et al. 2008) again suggests that the jet, rather than the accretion flow, dominates the X-ray emission. Nonetheless, only the combination of high effective area and simultaneous soft and hard band offered by *Suzaku* can resolve once and for all the issues surrounding the Fe $K\alpha$ line, as well as place strong limits on the luminosity of the accretion flow.

This paper is organized as follows. Section 2 provides a summary of our observations and a description of their reduction. In Section 3, we present the results of our spectral fitting to the XIS and HXD data. In Section 4, we show that an Fe $K\alpha$ line is not detected, while in Section 5 we discuss whether or not a buried AGN is present in NGC 6251. We end with our conclusions in Section 6.

2. OBSERVATIONS AND DATA REDUCTION

We observed NGC 6251 with *Suzaku* on 2010 December 02 (OBSID 705039010) for a nominal exposure of 87 ks. Both the X-ray Imaging Spectrometer (XIS) and Hard X-ray Detector (HXD) were operated in their normal modes. The source was positioned at the nominal aimpoint of the XIS instrument. The data were processed using v. 2.5.16.29 of the *Suzaku* processing pipeline, which includes the latest Charge Transfer Inefficiency (CTI) correction applied for the XIS. We used the standard cleaned events files, which are screened to remove periods during which the satellite passed through the South Atlantic Anomaly (SAA), had a pointing direction $<5^\circ$ above the Earth, or had Earth day-time elevation angles $<20^\circ$. We describe our analysis of the XIS and HXD data below.

2.1. XIS

We used data from the two operational front-illuminated (FI) CCDs (XIS0 and XIS3), together with the back-illuminated XIS1 detector. The three XIS CCDs were operated with a frame time of 8 s. For our analysis, we used data taken in the 3×3 and 5×5 edit modes. We selected only events corresponding to grades 0, 2, 3, 4, and 6, and removed hot and flickering pixels with the CLEAN SIS tool.

We extracted the spectrum of NGC 6251 from the XIS CCDs using a source-centered circle of radius $260''$ (250 physical pixels), with background sampled from an adjacent region free from any unrelated sources, as well as the ^{55}Fe calibration sources at the corners of each detector. We generated response matrix files (RMFs) for each detector using v. 2009-02-28 of the XISRMFGEN software, and ancillary response files (ARFs) using v. 2009-01-08 of the XISSIMARFGEN software.

The net exposure times and count rates for the three CCDs are shown in Table 1. We co-added the two FI spectra using the ADDASCASPEC program, and grouped the resulting spectrum and that of the XIS1 detector to a minimum of 50 counts per bin in order to use χ^2 statistics. We restricted the energy range for our spectral fitting to 0.5–10 keV.

2.2. HXD

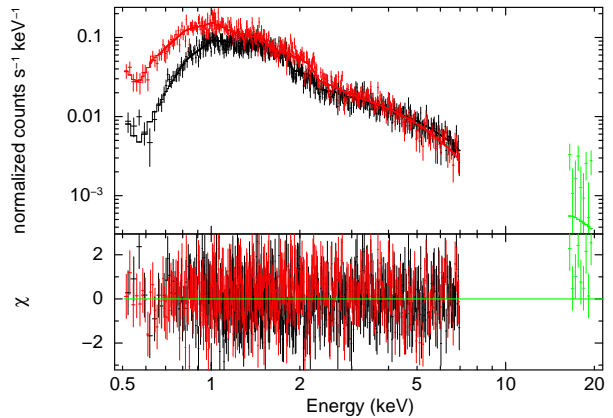


FIG. 1.— *Suzaku* XIS FI (black), XIS BI (red), and HXD PIN (green) best-fitting spectra and residuals. The model fit is the sum of a power law with slight excess absorption (consistent with the known dusty disk), and two collisionally ionized plasma components (**Model IV**).

We extracted the source spectrum from the HXD/PIN detector, using the cleaned PIN events files described above. The source was not detected with the GSO instrument. We used the HXD PINXBPI script, which generates the PIN non X-ray background (NXB) spectrum from the latest ‘tuned’ time-dependent instrumental background event file provided by the *Suzaku* Guest Observer Facility. The script also extracts the source and background spectra using a common Good Time Interval (GTI) criterion, creates a Cosmic X-ray Background (CXB) spectrum, and adds the CXB and NXB spectra together. We adopted the default binning criterion of 20 counts per channel. NGC 6251 is detected at energies between 16 and 20 keV, and so we restrict our subsequent spectral analysis to this range.

3. SPECTRAL ANALYSIS

In all spectral fits, we linked the parameters of the model components across the *Suzaku* XIS FI, XIS BI, and HXD PIN spectra. We tied the normalizations of the FI and BI XIS spectra together, but applied a constant cross-normalization factor of 1.16 for the PIN spectrum relative to the XIS as described in the *Suzaku* Data Reduction Guide⁶. We performed our spectral fitting using v.12.6.0 of the XSPEC spectral fitting package. All results presented here use a cosmology in which $\Omega_{m,0} = 0.3$, $\Omega_{\Lambda,0} = 0.7$, and $H_0 = 70 \text{ km s}^{-1} \text{ Mpc}^{-1}$. At the redshift of NGC 6251, $z=0.02471$, the luminosity distance is 267.3 Mpc. Errors quoted are 90 per cent confidence for one parameter of interest (i.e., $\chi^2_{\text{min}} + 2.7$), unless otherwise stated. All spectral fits include the Galactic absorption to NGC 6251 of $N_{\text{H,Gal}} = 1.69 \times 10^{20} \text{ cm}^{-2}$ (Dickey & Lockman 1990).

We initially attempted to model the spectrum using a single, unabsorbed power law, but this resulted in a poor fit ($\chi^2=1034$ for 832 dof) and noticeable residuals around 1 keV (**Model I**) that suggested the need for a thermal component. Following the methods of Guainazzi et al. (2003), Gliozzi et al. (2004), and Evans et al. (2005), we subsequently added a collisionally ionized plasma (APEC) component with its abundance fixed at 0.35 of solar (similar to Evans et al. 2005), which resulted in a substantial improvement to the fit ($\Delta\chi^2=134$ for 2 additional parameters), but still gave significant residuals below 1 keV (**Model II**). Next, we added a second APEC component to the model, which improved the fit to $\chi^2=871$ for 828 dof (**Model**

⁶ <http://heasarc.gsfc.nasa.gov/docs/suzaku/analysis/abc/>

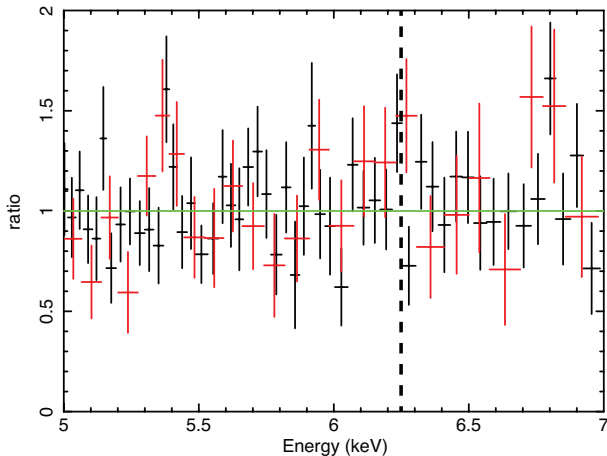


FIG. 2.— *Suzaku* FI (black) and BI (red) data/model ratio in the energy range 5–7 keV. Also marked is the position where a neutral Fe $K\alpha$ line would lie (dashed line).

III. Finally, owing to this model’s overprediction of flux below 0.7 keV, we added neutral intrinsic absorption at the redshift of NGC 6251 to the power law component (**Model IV**). This resulted in a substantial improvement to the fit ($\Delta\chi^2=33$ for 1 additional parameter). The best-fitting spectrum and model are shown in Figure 1. The addition of additional components, such as heavily obscured emission, failed to provide a significant improvement to the fitting statistic, and so we adopt Model IV as our best fit in the following discussion.

The measured intrinsic absorption is $N_{\text{H}}=(7.68^{+1.26}_{-2.18}) \times 10^{20} \text{ cm}^{-2}$. The detection of modest absorption at the redshift of NGC 6251 is not surprising, given the known dusty disk in the host galaxy. Indeed, the visual extinction of $A_V = 0.61 \pm 0.12$ mag (Ferrarese & Ford 1999) corresponds to a neutral hydrogen column density of $(1.3 \pm 0.3) \times 10^{21} \text{ cm}^{-2}$, which is close to the measured value from the *Suzaku* spectrum. The power law photon index of $\Gamma=1.82^{+0.04}_{-0.05}$ is consistent with the range of values from other X-ray observatories presented by Evans et al. (2005). The 2–10 keV unabsorbed luminosity of the power law is $(2.78^{+0.17}_{-0.24}) \times 10^{42} \text{ ergs s}^{-1}$, which again is within the range of historical values discussed by Evans et al. (2005). We also detect two collisionally ionized plasmas, with temperatures $0.80 \pm 0.15 \text{ keV}$ and $kT=1.42^{+0.45}_{-0.20} \text{ keV}$. Their temperatures are consistent with the extended emission detected by *XMM-Newton* on scales of tens and hundreds of kpc, respectively (Sambruna et al. 2004; Evans et al. 2005). Furthermore, the fraction of the integrated luminosity of the beta profile determined by Evans et al. (2005) within our 260'' *Suzaku* extraction region is approximately 60%. This corresponds to a bolometric luminosity of $4.4 \times 10^{41} \text{ ergs s}^{-1}$, which is consistent with the luminosity we measure with *Suzaku*.

4. NO EVIDENCE OF IRON $K\alpha$ EMISSION

A key goal of our *Suzaku* observation was to search for Fe $K\alpha$ emission, which would indicate the presence of reflection from an accretion disk, and/or circumnuclear torus. Figure 2 shows the XIS FI and BI data/model ratios of NGC 6251 in the energy range 5–7 keV. It is immediately evident that no Fe $K\alpha$ line is detected with *Suzaku*. Nonetheless, we added to our best-fitting spectral model a Gaussian line with its energy fixed at 6.4 keV and its width fixed at 50 eV (below the instrumental resolution of XIS). This resulted in a small improvement to the fit ($\Delta\chi^2=1.38$ for 1 additional parameter), with

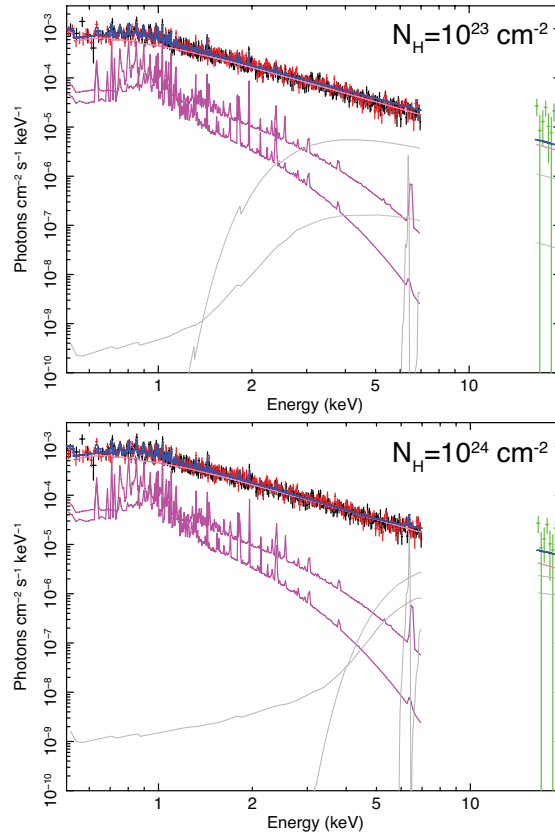


FIG. 3.— *Suzaku* XIS FI (black), XIS BI (red), and HXD PIN (green) unfolded spectra. The overall model fit shown (blue) consists of an absorbed power law (pink) and two thermal components (maroon), plus the direct, reflected, and fluorescent components of MYTorus (gray). We have assumed a column density of 10^{23} cm^{-2} (upper panel) and 10^{24} cm^{-2} (lower panel). The absorbed power law had a best-fit normalization of 0, but for illustrative purposes we show its 3σ upper limit. In both cases, we assumed that there were no systematic uncertainties in the PIN background.

a probability of 24% that the improvement is due to statistical fluctuations alone. The lower limit to the normalization of the Gaussian is consistent with zero, while the upper limit to the equivalent width (with respect to the overall continuum) is $\sim 100 \text{ eV}$. We therefore conclude that there is no substantial evidence for neutral Fe $K\alpha$ emission, although we caution that we cannot rule out its presence entirely.

5. IS A BURIED AGN PRESENT IN NGC 6251?

We next used the entire *Suzaku* bandpass to search for the presence of any signatures related to an accretion flow and torus. We assumed that, in addition to the dominant power-law component (which Evans et al. 2005 interpreted to be associated with a jet), there exists a “buried”, highly obscured AGN. We added to our best-fitting spectral description the MYTorus table models (Murphy & Yaqoob 2009), a fully self-consistent treatment of reflection and absorption from a circumnuclear torus. Specifically, MYTorus includes components that represent the (absorbed) zero-order continuum, the scattered continuum, and resulting neutral fluorescent lines. We assumed (1) the primary (accretion-related) power law has a photon index of 1.7 (consistent with the mean photon index of $z < 0.1$ 3CRR sources found by Evans et al. 2006); and (2) it is attenuated by equatorial column densities of 10^{23} cm^{-2} (consistent with HERGs measured by Evans et al. 2006 and Balmaverde et al. 2006) or 10^{24} cm^{-2} (to test the Compton-thick case). The choice of inclination angle is problematic:

Jones & Wehrle (2002) used the jet-counterjet brightness ratio to conclude that the angle to the line of sight, θ , of the jet is $\lesssim 45^\circ$, but this is different to that subtended by the dusty disk (76°) (Ferrarese & Ford 1999). For illustrative purposes, we adopt an angle of 90° (i.e., an edge-on geometry) and note that our results are essentially unaffected by the choice of angle until $\theta < 60^\circ$, after which the reprocessor adopted by Murphy & Yaqoob (2009) no longer intersects our line of sight.

The XIS and HXD spectra and models for the 10^{23} cm^{-2} and 10^{24} cm^{-2} cases are shown in Figure 3. The best-fitting accretion-related power law normalizations were consistent with zero, with 3σ upper limits to the 2–10 keV unabsorbed luminosity of $7 \times 10^{41} \text{ ergs s}^{-1}$ and $4 \times 10^{42} \text{ ergs s}^{-1}$, respectively. Assuming a black hole mass of $6 \times 10^8 M_\odot$ (Ferrarese & Ford 1999), we find that any obscured, accretion-related emission is highly sub-Eddington ($L_X/L_{\text{Edd}} \lesssim 10^{-5}$ for $N_{\text{H}}=10^{23} \text{ cm}^{-2}$; $L_X/L_{\text{Edd}} \lesssim 5 \times 10^{-5}$ for $N_{\text{H}}=10^{24} \text{ cm}^{-2}$). The upper limit to the 2–10 keV luminosity in both cases is consistent with the relationship between X-ray luminosity and $15\mu\text{m}$ luminosity established by Hardcastle et al. (2009).

As an additional test, we considered an extreme Compton thick obscurer ($N_{\text{H}}=10^{25} \text{ cm}^{-2}$). Again, this failed to provide a significant improvement to the fit. The upper limit to the 2–10 keV unabsorbed luminosity in this case is $2 \times 10^{44} \text{ ergs s}^{-1}$. However, we note that (1) the peak of the Compton reflection hump lies outside of the usable energy range of the PIN data, meaning that the principal feature used to determine the strength of the accretion-related emission is inaccessible, and (2) a luminosity of $2 \times 10^{44} \text{ ergs s}^{-1}$ would be a 6σ outlier from the Hardcastle et al. (2009) $L_X-L_{15\mu\text{m}}$ relationship. Observations with *NuSTAR* and *Astro-H* would provide further constraints.

Finally, given the poor signal-to-noise of our PIN data, it is important to address the known systematic uncertainties of the *Suzaku* background, which are of order 3% at the 1-sigma level (Fukazawa et al. 2009). In the above analysis, we noticed several points in the PIN band that appear to lie above the model. However, increasing the background by 3% (set using the cornorm parameter in XSPEC) removes any discrep-

ancy, ruling out any evidence of a hard excess given the PIN systematics.

6. CONCLUSIONS

We have presented results from a new 87-ks *Suzaku* observation of the prototypical low-excitation radio galaxy NGC 6251. We have shown the following:

1. We model the 0.5–20 keV *Suzaku* spectrum with a single power law of photon index $\Gamma = 1.82_{-0.05}^{+0.04}$, together with two collisionally ionized plasma models whose parameters are consistent with the known galaxy- and group-scale thermal emission.
2. There is no significant evidence in the X-ray for obscured, accretion-related emission. However, we cannot rule out accretion-flow luminosities of $< 7 \times 10^{41} \text{ ergs s}^{-1}$ and $4 \times 10^{42} \text{ ergs s}^{-1}$ if they are obscured by columns of 10^{23} cm^{-2} or 10^{24} cm^{-2} , respectively. These luminosities are consistent with those predicted by the $L_X-L_{15\mu\text{m}}$ relationship established by Hardcastle et al. (2009). Both luminosities are highly sub-Eddington ($L_X/L_{\text{Edd}} \sim 10^{-5}$).
3. NGC 6251 is thus consistent with our predictions for low-excitation radio galaxies: they have radiatively inefficient accretion flows, show no evidence in the X-ray for circumnuclear tori, and their X-ray emission is likely to be jet-dominated in nature.

We wish to thank the anonymous referee for providing constructive comments. DAE gratefully acknowledges financial support for this work from NASA under grant number NNX11AD34G. This research has made use of data obtained from the *Suzaku* satellite, a collaborative mission between the space agencies of Japan (JAXA) and the USA (NASA). This research has also used the NASA/IPAC Extragalactic Database (NED) which is operated by the Jet Propulsion Laboratory, California Institute of Technology, under contract with NASA.

REFERENCES

- Balmaverde, B., Capetti, A., & Grandi, P. 2006, *A&A*, 451, 35
 Chiaberge, M., Gilli, R., Capetti, A., Macchetto, F. D. 2003, *ApJ*, 597, 166
 Dickey, J. M., & Lockman, F. J. 1990, *ARA&A*, 28, 215
 Evans, D. A., Hardcastle, M. J., Croston, J. H., Worrall, D. M., & Birkinshaw, M. 2005, *MNRAS*, 359, 363
 Evans, D. A., Worrall, D. M., Hardcastle, M. J., Kraft, R. P., & Birkinshaw, M. 2006, *ApJ*, 642, 96
 Ferrarese, L., & Ford, H. C. 1999, *ApJ*, 515, 583
 Fukazawa, Y., Mizuno, T., Watanabe, S., et al. 2009, *PASJ*, 61, 17
 Garofalo, D., Evans, D. A., & Sambruna, R. M. 2010, *MNRAS*, 406, 975
 George, I. M., & Fabian, A. C. 1991, *MNRAS*, 249, 352
 Gliozzi, M., Sambruna, R. M., Brandt, W. N., Mushotzky, R., & Eracleous, M. 2004, *A&A*, 413, 139
 Gliozzi, M., Papadakis, I. E., & Sambruna, R. M. 2008, *ApJ*, 678, 78
 Guainazzi, M., Grandi, P., Comastri, A., Matt, G. 2003, *A&A*, 410, 131
 Hardcastle, M. J., Evans, D. A., & Croston, J. H. 2007a, *MNRAS*, 376, 1849
 Hardcastle, M. J., Evans, D. A., & Croston, J. H. 2009, *MNRAS*, 396, 1929
 Ho, L. C., 1999, *ApJ*, 516, 672
 Jones, D. L., & Wehrle, A. E. 2002, *ApJ*, 580, 114
 Kraft, R. P., Birkinshaw, M., Hardcastle, M. J., Evans, D. A., Croston, J. H., Worrall, D. M., & Murray, S. S. 2007, *ApJ*, 659, 1008
 Migliori, G., Grandi, P., Torresi, E., Dermer, C., Finke, J., Celotti, A., Mukherjee, R., Errando, M., Gargano, F., Giordano, F., & Giroletti, M. 2011, *A&A*, accepted (preprint arXiv:1107.4302)
 Murphy, K. D., & Yaqoob, T. 2009, *MNRAS*, 397, 1549
 Ogle, P., Whysong, D., & Antonucci, R. 2006, *ApJ*, 647, 161
 Sambruna, R. M., Gliozzi, M., Donato, D., Tavecchio, F., Cheung, C. C., & Mushotzky, R. F. 2004, *A&A*, 414, 885
 Smolčić, V. 2009, *ApJ*, 699, L43
 Tasse, C., Best, P. N., Röttgering, H., & Le Borgne, D. 2008, *A&A*, 490, 893
 Turner, T. J., George, I. M., Nandra, K., & Mushotzky, R. F. 1997, *ApJS*, 113, 23

TABLE 1
SUZAKU OBSERVATION LOG

Date of observation	Obs. ID	Instrument	Screened exposure time	Net nuclear count rate (s^{-1})
2010 Dec 02	705039010	XIS0	87 ks	0.15 ± 0.02
		XIS1	87 ks	0.21 ± 0.02
		XIS3	87 ks	0.16 ± 0.02
		HXD/PIN	74 ks	$(6.46 \pm 1.18) \times 10^{-2}$

TABLE 2
BEST-FITTING SPECTRAL PARAMETERS

Model	Description	N_H (cm^{-2})	Power Law	Thermal 1	Thermal 2	χ^2/dof
I	PL		$\Gamma = 1.87 \pm 0.02$ norm = $(6.79 \pm 0.09) \times 10^{-4}$			1034/832
II	PL+TH1		$\Gamma = 1.75 \pm 0.03$ norm = $(5.62 \pm 0.22) \times 10^{-4}$	$kT = 1.21^{+0.07}_{-0.10}$ keV Z = 0.35 (f) norm = $(3.17 \pm 0.65) \times 10^{-4}$		900/830
III	PL+TH1+TH2		$\Gamma = 1.62^{+0.07}_{-0.09}$ norm = $(3.76^{+0.62}_{-0.79}) \times 10^{-4}$	$kT = 0.89 \pm 0.10$ keV Z = 0.35 (f) norm = $(2.04^{+0.48}_{-0.42}) \times 10^{-4}$	$kT = 2.63^{+0.69}_{-0.47}$ keV Z = 0.35 (f) norm = $(7.86^{+2.26}_{-2.36}) \times 10^{-4}$	871/828
IV	ABS(PL)+TH1+TH2	$(7.68^{+1.26}_{-2.18}) \times 10^{20}$	$\Gamma = 1.82^{+0.04}_{-0.05}$ norm = $(6.17^{+0.38}_{-0.54}) \times 10^{-4}$	$kT = 0.80 \pm 0.15$ keV Z = 0.35 (f) norm = $(1.27^{+0.38}_{-0.63}) \times 10^{-4}$	$kT = 1.42^{+0.45}_{-0.20}$ keV Z = 0.35 (f) norm = $(2.22^{+1.04}_{-0.66}) \times 10^{-4}$	838/827

^aCol. (1): Model number. Col. (2): Description of spectrum (Abs=Neutral absorption, PL=Power Law, TH=Collisionally ionized plasma model). Col. (3): Intrinsic neutral hydrogen column density. Galactic absorption has also been applied. Col. (4): Power Law parameters. Normalization is quoted at 1 keV in units of $ph\ keV^{-1}\ cm^{-2}\ s^{-1}$. Col. (5): Parameters of first collisionally ionized plasma model. Col. (6): Parameters of second collisionally ionized plasma model. Col. (7): Value of χ^2 and degrees of freedom.